Geological Magazine

Life cycle analysis of coesite-bearing garnet by Jan Schönig, Hilmar von Eynatten, Guido Meinhold, and N. Keno Lünsdorf

Supplementary Material 2:

Detailed information on garnet grains containing specific inclusion types

SM2a: Rutile-bearing garnet

Rutile, the most frequent inclusion type, occurs in garnet of all compositions (Fig. SM2a). Comparing the kernel density plots of rutile-bearing garnet grains with that of all inclusion-bearing garnet grains (Fig. 3), the distribution pattern is rather similar and there are only minor variations with rutile-bearing garnet being slightly more frequent in garnet from high-grade metamorphic sources. Between the samples, there is a minor variation with regard to rutile-bearing garnet abundance and most samples show amounts ~60 %, except JS-Erz-3s which shows a significantly lower frequency (Fig. SM2a, bar chart). However, rutile-bearing garnet frequency and source rock composition do not correlate because samples from catchments being dominated by felsic rocks (JS-Erz-8s, JS-Erz-9s, and JS-Erz-13s) as well as catchments with higher proportions of eclogite (JS-Erz-3s, JS-Erz-5s, and JS-Erz-6s) internally show significant variation in rutile-bearing garnet frequency.

In the ternary grain-size distribution plot of rutile-bearing garnet in Figure SM2a, it is shown that rutile-bearing garnet is slightly enriched in the 125–250 µm and even more in the 250–500 µm fraction compared to the 63–125 µm fraction. In addition, samples having lower abundancies in rutile-bearing garnet (JS-Erz-3s, JS-Erz-5s, and JS-Erz-8s) are even more enriched in the coarse fractions. Thus, it can be concluded that the amount of garnet containing a specific inclusion type generally increases with increasing grain size and that this source rock independent effect is more

pronounced for inclusion types occurring in lower proportions. This effect is caused by the increasing garnet volume analyzed with increasing grain size, making it more likely to contain a specific inclusion type, in particular when the inclusion frequency of this mineral phase is rather low.

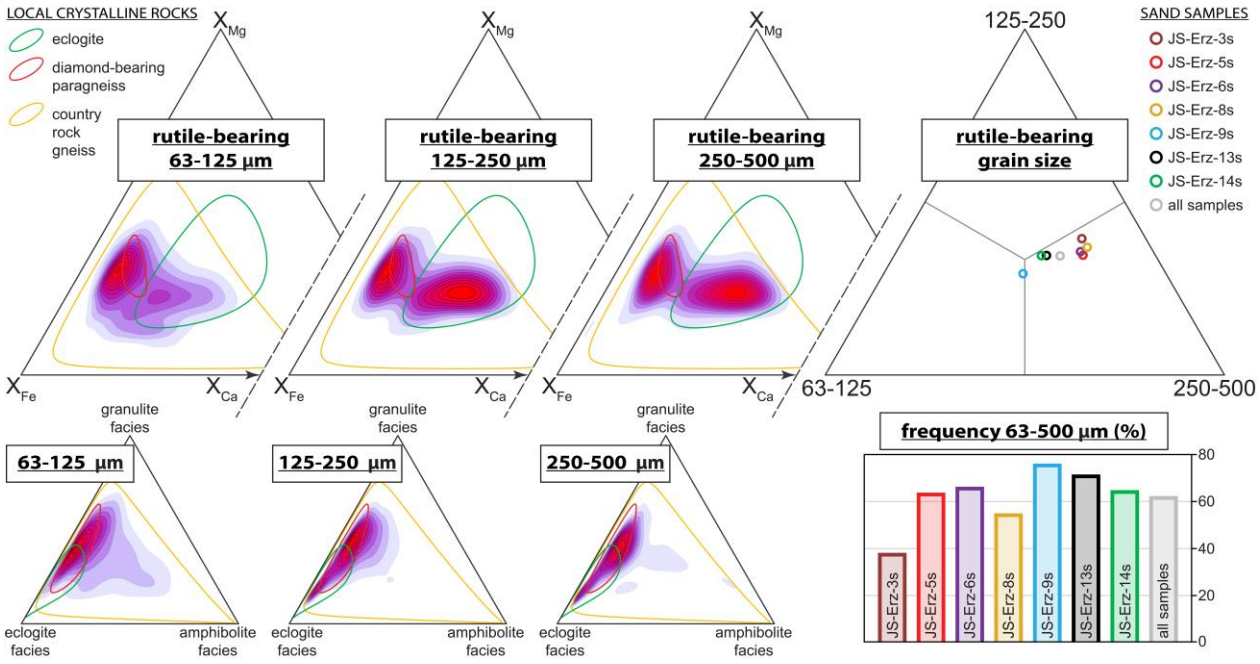

Figure SM2a: Composition, grain-size distribution, and frequency of rutile-bearing detrital garnet. Compositional distributions are shown for the three grain-size fractions as kernel density estimate heatmaps in the X_{Fe}– X_{Mg}–X_{Ca} ternary plots and in the probability ternary plots of metamorphic garnet after multivariate discrimination (Tolosana-Delgado *et al.* 2018). See SM1 for the dataset. For comparison, garnet composition of local crystalline rocks compiled by Schönig *et al.* (2020) are shown as 95 % confidence ellipsoids. Grain-size distributions of rutile-bearing garnet for the individual samples are illustrated in a ternary plot showing relative proportions for the number of grains in each analyzed grain-size fraction. The frequencies of rutile-bearing garnet for the individual samples of the entire analyzed grain-size window of 63–500 µm are shown in a bar plot.

SM2b: Omphacite-bearing garnet

Omphacite co-existing with garnet is the diagnostic mineral assemblage of eclogite-facies metamorphism. Potentially, omphacite-bearing garnet could derive from felsic eclogite-facies rocks but in the investigated area–omphacite inclusions in garnet as well symplectites after omphacite in felsic rocks occur occasionally (Willner *et al.* 1997). Thus, omphacite-bearing garnet seems to be an appropriate indicator for the mafic high-grade source rocks (i.e. eclogites), which

is supported by the composition of detrital garnet grains containing omphacite, which–almost exclusively matching with the 95 % confidence ellipsoid for the composition of garnet from local eclogite (Fig. SM2b). Only in the 63–125 µm fraction minor proportions of omphacite-bearing garnet point to felsic affinity.

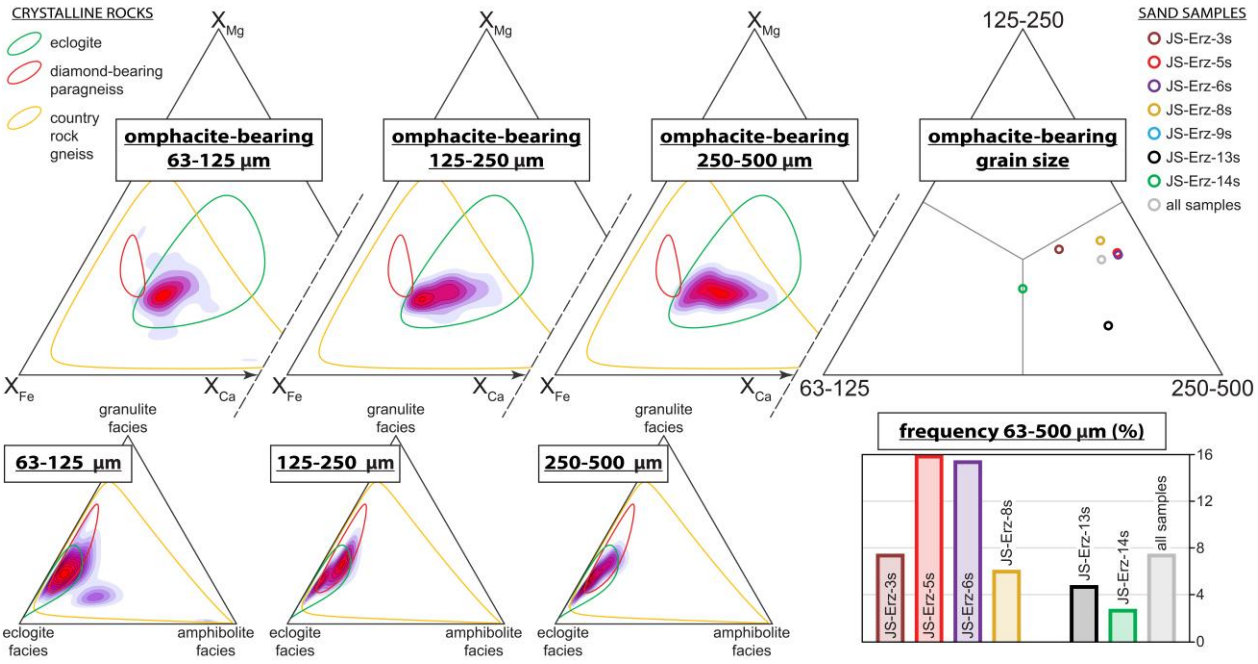

Figure SM2b: Composition, grain-size distribution, and frequency of omphacite-bearing detrital garnet. Compositional distributions are shown for the three grain-size fractions as kernel density estimate heatmaps in the X_{Fe}– X_{Mg}–X_{Ca} ternary plots and in the probability ternary plots of metamorphic garnet after multivariate discrimination (Tolosana-Delgado *et al.* 2018). See SM1 for the dataset. For comparison, garnet composition of local crystalline rocks compiled by Schönig *et al.* (2020) are shown as 95 % confidence ellipsoids. Grain-size distributions of omphacite-bearing garnet for the individual samples are illustrated in a ternary plot showing relative proportions for the number of grains in each analyzed grain-size fraction. The frequencies of omphacite-bearing garnet for the individual samples of the entire analyzed grain-size window of 63–500 µm are shown in a bar plot.

Considering the frequency of garnet grains containing omphacite inclusions, the high proportion of eclogite occurring in the catchments of samples JS-Erz-3s, JS-Erz-5s, and JS-Erz-6s is well-reflected, although JS-Erz-3s shows lower amounts than the two latter (Fig. SM2b, bar plot). In contrast, the dominantly felsic composition of country rocks in catchments from samples JS-Erz-8s, JS-Erz-9s, and JS-Erz-13s is reflected by lower omphacite-bearing garnet frequencies, although JS-Erz-8s shows higher amounts than the latter two. In addition, the dilution effect by garnet grains

from lower-grade metamorphic rocks in sample JS-Erz-14s as implied by garnet chemistry (see Section 4.a.) is also supported by low proportions of omphacite-bearing garnet. In the grain-size distribution plot of omphacite-bearing garnet in Figure SM2b, it is clearly indicated that garnet containing omphacite is enriched in the coarse fraction independently from the proportion of eclogite occurring in the catchment. This agrees with previous observations of an increasing metamorphic grade with increasing garnet grain size (Fig. 1), and the typical large garnet crystal size in eclogite leading to a grain-size inheritance effect.

SM2c: Graphite-bearing garnet

Contrary to omphacite-bearing garnet, garnet containing inclusions of graphite are a characteristic feature of felsic para-metamorphic rocks. This is supported by their compositional variation covering the entire range of local felsic rocks and only marginally overlap with that of eclogite reflecting the general compositional overlap of felsic and eclogitic rocks (Fig. SM2c). Graphite-bearing garnet frequency correlates negatively with that of omphacite-bearing garnet, and thus again well reflect the geological framework of the catchments (Fig. SM2c, bar plots). Compared to the grain-size distributions of rutile- and omphacite-bearing garnet, which internally have a quite similar pattern for almost all samples, graphite-bearing garnet in the individual samples show strong variations regarding grain size (cf. Figs. SM2a–SM2c, grain-size plots). Samples JS-Erz-9s, JS-Erz-13s, and JS-Erz-14s show an increase of graphite-bearing garnet with increasing grain size. In contrast, in particular sample JS-Erz-6s but also JS-Erz-3s, JS-Erz-5s, and JS-Erz-8s show enrichment of graphite-bearing garnet in the 63–125 µm fraction. These grain-size relations are caused by the dominant occurrence of omphacite-bearing garnet in the coarse fractions (125–250 and 250–500 µm) diluting the amount of graphite-bearing garnet. Samples containing minor amounts of omphacite-bearing garnet due to the low proportion of eclogitic sources, i.e. JS-Erz-9s,

JS-Erz-13s, and JS-Erz-14s, show an increase of graphite-bearing garnet with increasing grain size due to the larger garnet volume analyzed as discussed for rutile-bearing garnet (see above). In contrast, samples containing higher amounts of omphacite-bearing garnet like JS-Erz-5s and JS-Erz-6s, but also JS-Erz-3s and JS-Erz-8s, show enrichment of graphite-bearing garnet in the 63–125 µm fraction. This dilution effect can be best observed by following the development of omphacite- and graphite-bearing garnet from sample JS-Erz-8s (upstream) to sample JS-Erz-6s (downstream, Fig. 2b). Compared to the other samples, JS-Erz-8s shows an intermediate amount of omphacite-bearing garnet enriched in the coarse fractions and an intermediate amount of graphite-bearing garnet slightly enriched in the fine fraction (Figs. SM2b and SM2c). Farther downstream, the catchment of the sampled creek drains a large eclogite body at its western site leading to a significant increase of omphacite-bearing garnet in JS-Erz-6s being even stronger enriched in the coarse fraction (Fig. SM2b), and a decrease of graphite-bearing garnet being highly enriched in the fine fraction (Fig. SM2c).

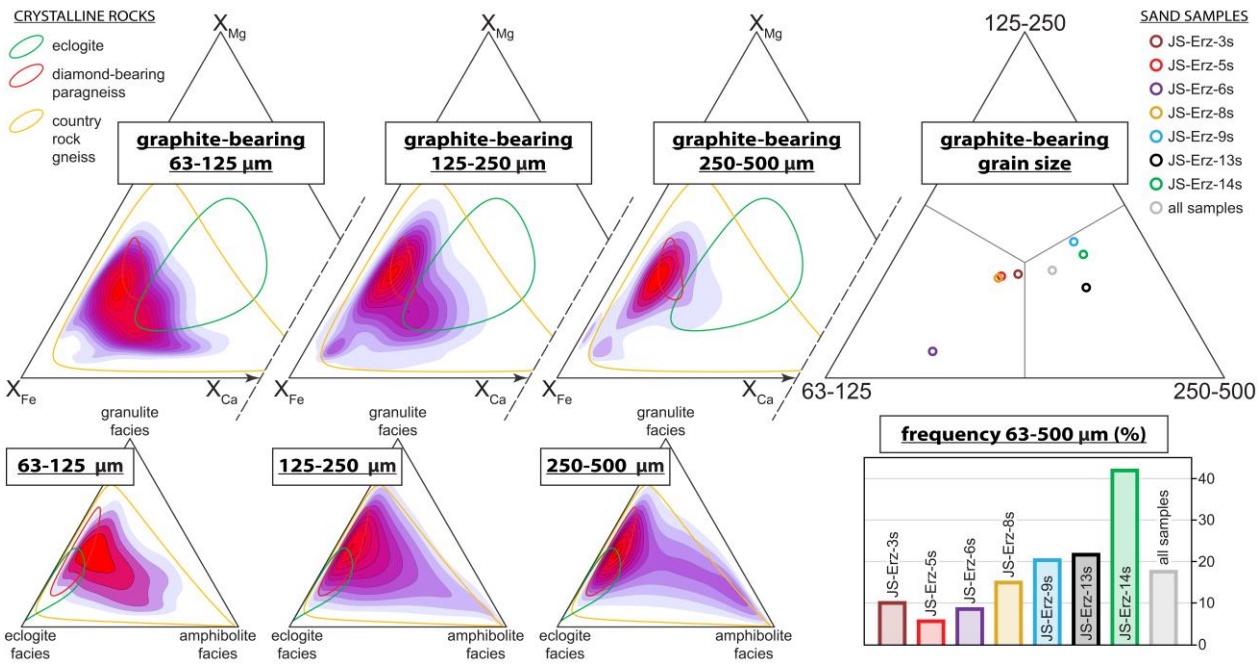

Figure SM2c: Composition, grain-size distribution, and frequency of graphite-bearing detrital garnet. Compositional distributions are shown for the three grain-size fractions as kernel density estimate heatmaps in the X_{Fe}– X_{Mg}–X_{Ca} ternary

plots and in the probability ternary plots of metamorphic garnet after multivariate discrimination (Tolosana-Delgado *et al.* 2018). See SM1 for the dataset. For comparison, garnet composition of local crystalline rocks compiled by Schönig *et al.* (2020) are shown as 95 % confidence ellipsoids. Grain-size distributions of graphite-bearing garnet for the individual samples are illustrated in a ternary plot showing relative proportions for the number of grains in each analyzed grain-size fraction. The frequencies of graphite-bearing garnet for the individual samples of the entire analyzed grain-size window of 63–500 µm are shown in a bar plot.

SM2d: Quartz- and kyanite-bearing garnet

As graphite-bearing garnet represents the entire range of exclusively felsic sources and its grain-size distribution is highly affected by the proportion of eclogitic source rocks (see above), graphite-bearing garnet is not suitable to evaluate the grain-size distribution of garnet from lower grade felsic sources, i.e. country rock gneiss, compared to high-grade felsic sources similar to the diamond-bearing paragneiss. For that, the distribution of garnet containing inclusions of quartz and kyanite are more suitable. Both inclusion types are mainly a feature of the felsic sources (e.g. Willner *et al.* 1997; Nasdala & Massonne, 2000), which is supported by garnet chemistry from all grain-size fractions (Fig. SM2d). However, both types subordinately also occur in eclogite (e.g. Schmädicke *et al.* 1992; Gose & Schmädicke, 2018), as supported by smaller populations matching with the composition of garnet from local eclogite (Fig. SM2d). Thus, quartz- and kyanite-bearing garnet mainly represent felsic sources and their grain-size distribution is less affected by varying proportions of eclogitic sources. In addition, detrital garnet composition reveals that the amount of quartz-bearing garnet is more pronounced for lower-grade felsic sources (i.e. country rock gneisses, Fig. SM2d A), whereas the amount of kyanite-bearing garnet is more pronounced for high-grade felsic sources (Fig. SM2d B).

Considering the frequency of quartz-bearing garnet, it again well reflects the dominantly felsic framework of the catchments from samples JS-Erz-9s, JS-Erz-13s, and JS-Erz-14s (Fig. SM2d A, bar plot), as already shown by the frequency of graphite-bearing garnet (Fig. SM2c, bar plot). In contrast, the frequency of kyanite-bearing garnet is more heterogeneous and indicates significant inputs from high-grade felsic source rocks for samples JS-Erz-3s and especially JS-Erz-8s, but also

for JS-Erz-13s. Obviously, the grain-size distribution plots show enrichment of quartz-bearing garnet in the 63–125 µm fraction overcoming the effect of the increasing garnet volume analyzed

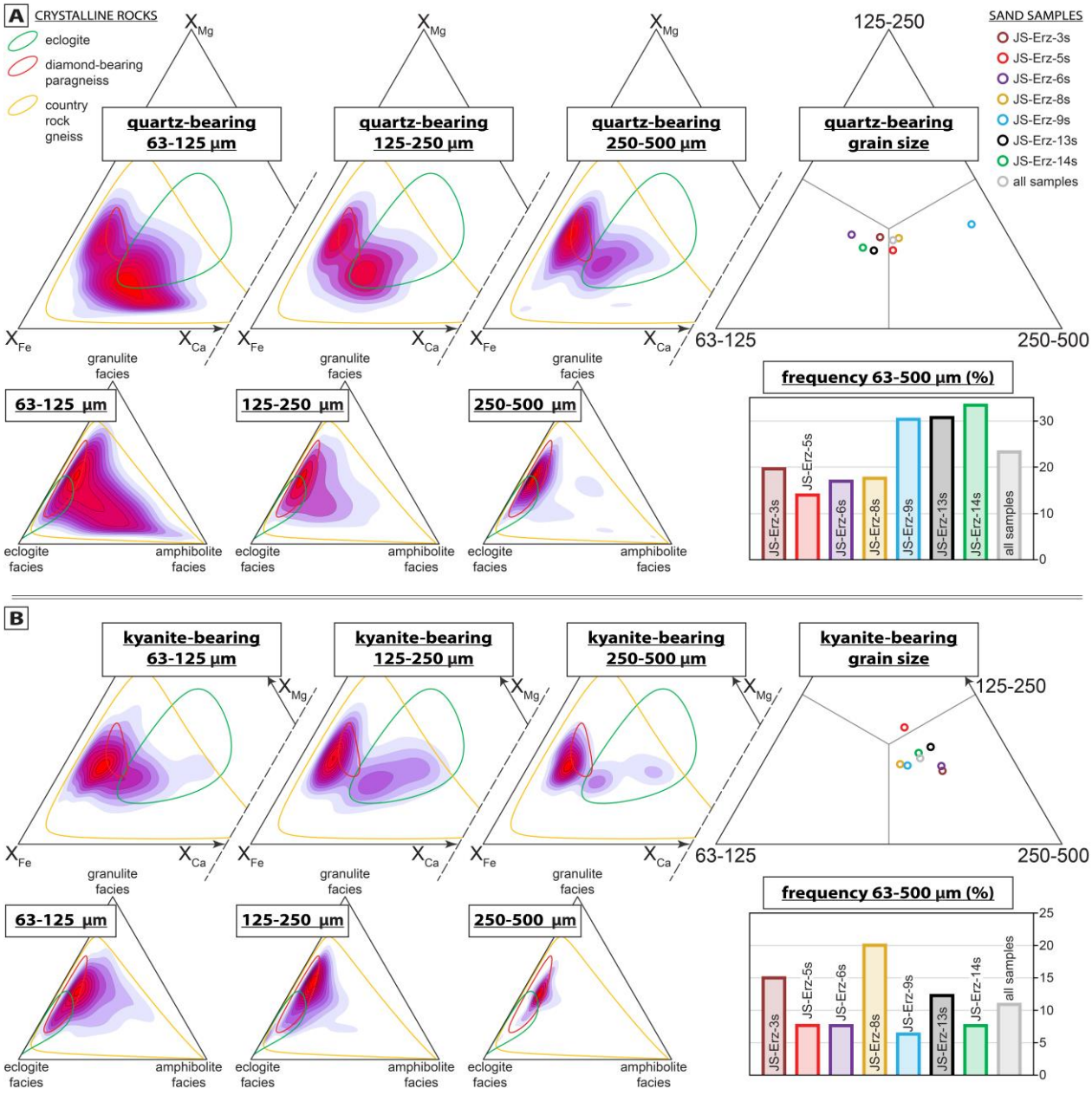

Figure SM2d: Composition, grain-size distribution, and frequency of (A) quartz- and (B) kyanite-bearing detrital garnet. Compositional distributions are shown for the three grain-size fractions as kernel density estimate heatmaps in the X_{Fe}–X_{Mg}–X_{Ca} ternary plots and in the probability ternary plots of metamorphic garnet after multivariate discrimination (Tolosana-Delgado *et al.* 2018). See SM1 for the dataset. For comparison, garnet composition of local crystalline rocks compiled by Schönig *et al.* (2020) are shown as 95 % confidence ellipsoids. Grain-size distributions of quartz- and kyanite-bearing garnet for the individual samples are illustrated in ternary plots showing relative proportions for the number of grains in each analyzed grain-size fraction. The frequencies of quartz- and kyanite-bearing garnet for the individual samples of the analyzed grain-size window of 63–500 µm are shown in bar plots.

with increasing grain size, except for garnet of sample JS-Erz-9s which is exclusively shed from homogeneous felsic rocks (Fig. SM2d A). In contrast, kyanite-bearing garnet is clearly enriched in the coarsest fraction (Fig. SM2d B). Thus, it can be concluded that high-grade metamorphic rocks of both mafic (see above) and felsic composition primarily supply large garnet crystals to the sedimentary system leading to an enrichment in the coarser detrital garnet fractions due to an inherited grain size from source to sink. Notably, sample JS-Erz-8s shows a similar grain-size distribution of quartz- and kyanite-bearing garnet contrary to all other samples, implying that another process controlling the grain-size distribution of this sample is involved.